# From SPS to RHIC: Breaking the Barrier to the Quark-Gluon Plasma

Ulrich Heinz

*Physics Department, The Ohio State University, Columbus, OH 43210, USA*
*Email: heinz@mps.ohio-state.edu*

**Abstract.** After 15 years of heavy-ion collision experiments at the AGS and SPS, the recent turn-on of RHIC has initiated a new stage of quark-gluon plasma studies. I review the evidence for deconfined quark-gluon matter at SPS energies and the recent confirmation of some of the key ideas by the new RHIC data. Measurements of the elliptic flow at RHIC provide strong evidence for efficient thermalization during the very early partonic collision stage, resulting in a well-developed quark-gluon plasma with almost ideal fluid-dynamical collective behaviour and a lifetime of several fm/$c$.

## I. THE QUARK-HADRON TRANSITION

Quantum Chromodynamics (QCD), the theory of strong interactions, predicts for strongly interacting bulk matter a phase transition from a gas of hadron resonances (HG) at low energy densities to a quark-gluon plasma (QGP) at high energy densities. The critical energy density $\epsilon_c$ is of the order of $1\,\mathrm{GeV/fm^3}$ . It can be reached by heating matter at zero net baryon density to a temperature of about $T_c \approx 170\,\mathrm{MeV}$, or by compressing cold nuclear matter to baryon densities of about $\rho_c \sim 3-10\,\rho_0$ (where $\rho_0 = 0.15\,\mathrm{fm}^{-3}$ is the equilibrium density), or by combinations thereof. A simple version of the phase diagram is shown in Fig. 1 [ 1].

By colliding heavy ions at high energies one hopes to create hadronic matter at energy densities above $\epsilon_c$. At lower energies (SIS @ $1\,A\,\mathrm{GeV}$), the nuclei are stopped, compressed and moderately heated. At higher energies (AGS @ $10\,A\,\mathrm{GeV}$ and SPS @ $160\,A\,\mathrm{GeV}$) one reaches higher temperatures, but the colliding nuclei are no longer completely stopped and the baryon chemical potential of the matter created at rest in the c.m.s. decreases. At the colliders RHIC ($\sqrt{s} = 200\,A$ GeV) and LHC ($\sqrt{s} = 5500\,A\,\mathrm{GeV}$) the baryon chemical potential is so small that one essentially simulates the nearly baryon-free hot hadronic matter of the early universe. If the matter thermalizes quickly at energy densities above $\epsilon_c$, it will pass through the *quark-hadron phase transition* as the collision fireball expands and cools.

Along the temperature axis at $\mu_B = 0$ our knowledge of the QCD phase diagram is based on hard theory (lattice QCD) [ 2], but for nonzero baryon density we must still rely on models interpolating between low-density hadronic matter, described by low-energy effective theories, and high-density quark-gluon plasma, described by perturbative QCD [ 1]. The uncertainties at high-baryon densities are thus relatively large (typically $\mathcal{O}(30-50\%)$). At zero baryon density, numerical simulations of QCD with 3 dynamical light quark flavors on the lattice are now available, and the systematic errors due to lattice discretization and continuum extrapolation are beginning to get small [ 2]. The critical temperature $T_c$ for real-life QCD is predicted as $T_c \approx 170\,\mathrm{MeV} \pm 10\%$ [ 2]. Near $T_c$ the energy density in units of $T^4$ changes dramatically by more than a factor of 10 within a very narrow temperature interval. Above $T \simeq 1.2\,T_c$, $\epsilon/T^4$ appears to settle at about 80% of the Stefan-Boltzmann value for an ideal gas of non-interacting quarks and gluons.

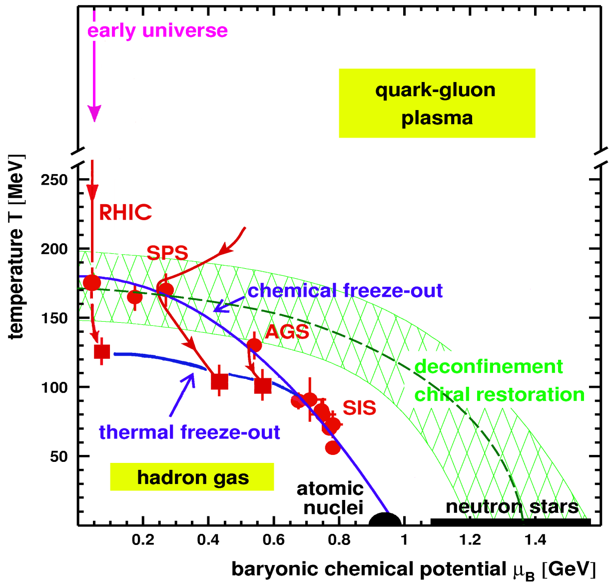


FIGURE 1. Sketch of the QCD phase diagram, temperature $T$ vs. the chemical potential $\mu_{\mathrm{B}}$ associated with net baryon density $\rho_{\mathrm{B}}$. The cross-hatched region indicates the expected phase transition and its present theoretical uncertainty, the dashed line representing its most likely location. Lines with arrows indicate expansion trajectories of thermalized matter created in different environments. For a discussion of the chemical and thermal freeze-out lines and the location of the data points see text.

According to lattice QCD, only about $0.6\,\mathrm{GeV/fm}^3$ of energy density are needed to make the transition to deconfined quark-gluon matter [ 2]. But it is very expensive to reach temperatures well above $T_c$: an initial temperature of 220 MeV, ≈30% above $T_c$, already requires an initial energy density $\epsilon \simeq 3.5\,\mathrm{GeV/fm}^3$, about 6 times the critical value. This limits severely the reach of the CERN SPS into the QGP phase: only the region at and slightly above $T_c$ can be probed. But with RHIC considerably higher energy densities have now become accessible so that we can penetrate deeper into the new phase. The situation will further improve with the beginning of the heavy-ion program at the LHC at CERN in 2007.

At $T_c$ two phenomena occur simultaneously [ 3]: color confinement is broken, i.e. colored degrees of freedom can propagate over distances much larger than the size of a hadron, and the approximate chiral symmetry of QCD, which is spontaneously broken at low temperatures and densities, gets restored. Both effects significantly accelerate particle production: the liberation of gluons in large densities opens up new gluonic production channels, and the threshold for quark-antiquark pair production is lowered due to the restoration of the spontaneously broken chiral symmetry at low densities.

## II. RECONSTRUCTING THE LITTLE BANG

As the two nuclei hit each other, a superposition of nucleon-nucleon (NN) collisions occurs. What is different from individual NN collisions is that (i) each nucleon scatters several times, and (ii) the partons liberated in different NN collisions rescatter with each other even before hadronization, as do the hadrons afterwards. Both change the particle production *per participating nucleon*, but only the rescattering processes can lead to a state of local thermal equilibrium, by redistributing the energy lost by the beams into the statistically most probable configuration. They cause thermodynamic pressure acting against the outside vacuum, and this makes the reaction zone expand collectively. *This is a genuine collective nuclear effect, with no analogue in elementary particle collisions.* The expansion dilutes the fireball below $\epsilon_c$, at which point hadrons are formed from the quarks and gluons (hadronization). Further interactions among these hadrons cease once their average distance exceeds the range of the strong interactions: the hadrons "freeze out".

The strong interactions among the partons and hadrons before freeze-out wipe out much information about their original production processes. Extracting information about the hot and dense early collision stage thus requires to exploit features which are either established early and survive the rescattering and collective expansion or can be reliably back-extrapolated. Correspondingly one classifies the observables into two classes, *early* and *late* signatures.

The conceptually cleanest early signatures are the directly produced real and virtual photons since these re-interact weakly and escape directly from the fireball (virtual photons materialize as $e^+e^-$ or $\mu^+\mu^-$ pairs). They are emitted throughout the expansion, but their production should be strongly weighted towards the hot and dense initial stages. Unfortunately, direct photons are rare, and the experimental background from hadronic decay photons after freeze-out is enormous.

Another early signature are hadrons containing charmed quarks. At the SPS, $c\bar{c}$ pairs can be only created in the primary NN collisions; secondary scatterings are already below the $c\bar{c}$ threshold. The latter can only redistribute them in phase-space, changing the relative amounts of mesons with hidden and open charm. It was shown that such a redistribution is much easier in the color-deconfined QGP phase than by reinteractions of charmed and other hadrons; in this way charm-redistribution becomes also an early signature. At SPS energies and below, charm production is a very rare process and only hidden charm mesons ($J/\psi, \psi'$) have been measured. The interpretation of what happens to them crucially depends on the assumption that no secondary charm is produced. At RHIC energies and above the production of additional charmed particles in secondary collisions becomes possible, and a consistent interpretation of charmonium data requires also the measurement of open charm. None of the present RHIC experiments can do that.

Hadrons made of $u$ and $d$ quarks can be easily produced and destroyed throughout the fireball expansion. Their abundances and spectra are *late signatures* which provide only *indirect* information about the early collision stages. But they are very numerous and can be measured very accurately. We'll use these *late* signals to reconstruct the Little Bang and then check the consistency of the resulting picture with the less detailed direct information from the *early* signals. Hadrons involving strange quarks play an intermediate role: $s\bar{s}$ pairs are easily produced in the dense color-deconfined, chirally almost symmetric QGP phase, but hadron interactions after hadronization leave their abundances essentially unaltered. Their yields thus reflect the situation reached at the quark-hadron transition point.

It was recently realized that in *non-central* collisions the observed collective flow pattern of *all* hadrons shows certain anisotropies ("elliptic flow") which are established very early in the collision, even before hadrons are formed, and are hardly changed in the late expansion stages. The elliptic flow of the emitted hadrons (including the abundant light ones) thus constitutes another *early collision signature*.

## III. INITIAL CONDITIONS

We can estimate the initially *produced* energy density by dividing the measured total transverse energy $E_T$ by an estimated initial reaction volume [ 4]

$$\epsilon_{\rm Bj}(\tau_0) = \frac{1}{\pi R^2}\,\frac{1}{\tau_0}\,\frac{dE_T}{dy}\,. \tag{1}$$

Here $\tau_0\, dy$ is an estimate for the length of a cylinder undergoing boost-invariant longitudinal expansion [ 4] from which particles with longitudinal momenta in a rapidity interval $dy$ are emitted. Inserting for $\pi R^2$ the overlap area of two Pb nuclei colliding at zero impact parameter, choosing $\tau_0 = 1\,{\rm fm}/c$, and using $dE_T/dy(y = 0) \approx 400\,{\rm GeV}$ for central Pb+Pb collisions [ 5] gives

$$\epsilon_{\rm Bj}^{\rm Pb+Pb}(1\,{\rm fm}/c) = 3.2 \pm 0.3\,{\rm GeV/fm}^3\,. \tag{2}$$

Note that this is the average over the transverse plane; the value $\epsilon_0 = \epsilon(r{=}0)$ in the center is about twice as high. The analogous value extracted from $\sqrt{s} = 130\,A\,{\rm GeV}$ Au+Au collisions at RHIC [ 6] is 60% larger, and recent PHOBOS data from $\sqrt{s} = 200\,A\,{\rm GeV}$ show another increase by about 15% [ 7]. As QGP searchers we are clearly playing in the right ball-park: if the matter were already thermalized after $1\,{\rm fm}/c$ (for which there is evidence from elliptic flow measurements, see below), the temperature corresponding to the SPS value (2) would be $T_0 \simeq 210-220\,{\rm MeV}$. At RHIC, thermalization seems to happen even earlier, at around 0.5-0.6 $\rm{fm}/c$ [ 8], and the initial temperature may have been as high as 350 MeV.

## IV. THERMAL FREEZE-OUT: AN EXPLODING FIREBALL

The measured hadron spectra contain two pieces of information: (i) Their normalizations, i.e. the *yields and abundance ratios*, provide the chemical composition of the fireball at the "chemical freeze-out" point where the hadron abundances freeze out; this gives information about the degree of chemical equilibration, see Sec. VI. (ii) The hadronic *momentum spectra* provide information about thermalization of the momentum distributions and collective flow. The latter is caused by thermodynamic pressure and thus reflects, in a time-integrated way, the equation of state of the fireball matter. We concentrate on the transverse flow since all of it is generated *during* the reaction.

In a thermal, collectively expanding system the shapes of *all* hadronic $m_\perp$-spectra ($m_\perp = \sqrt{m^2+p_\perp^2}$) can be characterized by just two numbers: the temperature $T_{\rm f}$ and the mean transverse flow velocity $\langle v_\perp \rangle$ at freeze-out. This is true if all hadrons decouple simultaneously, i.e. if their rescattering cross sections are similar. This can be checked experimentally: e.g., it was observed that the $\Omega$ [ 9] and $J/\psi$ [ 10] show steeper slopes than expected from the systematics of the remaining hadrons, because they have smaller hadronic rescattering cross sections and thus decouple earlier [ 11]. For all other hadrons, a common parametrization by a single pair $(T_{\rm f}, \langle v_\perp \rangle)$ works very well. The transverse flow velocity $\langle v_\perp \rangle$ manifests itself as a flattening of the $m_\perp$-spectra, by a mass-independent blueshift factor $T_{\rm slope} = T_{\rm f}\sqrt{(1+\langle v_\perp \rangle)/(1-\langle v_\perp \rangle)}$ in the relativistic domain $m_\perp > 2m_0$ and by a mass-dependent term $T_{\rm slope} = T_{\rm f} + \frac{1}{2} m_0 \langle v_\perp \rangle^2$ at small $p_\perp$. A roughly linear mass-dependence of the transverse slopes at low $p_\perp$ was observed at the SPS (see e.g. [ 9]). Fig. 2 shows that the RHIC data [ 12, 13] follow the same systematics, with antiproton spectra being much flatter at low $p_\perp$ than the pion spectra, in quantitative agreement with hydrodynamic calculations which assume complete thermalization of the fireball after $\tau_0 = 0.6\,{\rm fm}/c$ [ 14].

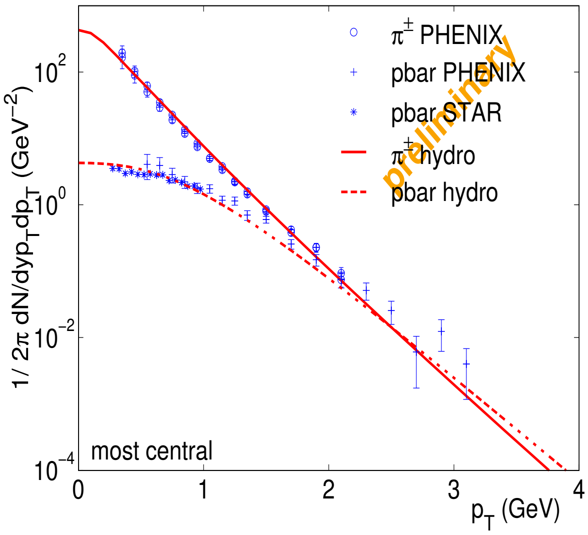


FIGURE 2. Preliminary transverse momentum spectra of charged pions and antiprotons from 130 $A$ GeV Au+Au collisions at RHIC [ 12, 13], compared with hydrodynamic predictions [ 14], corresponding to $T_{\rm f}$ = 128 MeV, $\mu_B$ = 70 MeV, and $\langle v_\perp \rangle$ = 0.6 $c$ (private communication by P.F. Kolb whom I thank for preparing this figure).

Transverse flow also affects two-particle momentum correlations and gives, for example, rise to a characteristic $m_\perp$-dependence of the source sizes extracted from Bose-Einstein correlation measurements [ 15] or deuteron yields [ 16, 17, 18]. The most accurate separation of thermal and collective contributions to the final hadron momenta is obtained from a simultaneous analysis of single-particle spectra and two-particle correlations [ 19, 20]. At the SPS this gives $T_{\rm f} \approx 100$ MeV and $\langle v_\perp \rangle \approx 0.55\,c$. The corresponding freeze-out energy density is only about 50 MeV/fm$^3$! For

RHIC such a combined analysis is not yet available, but the spectral slopes alone (see Fig. 2) indicate a somewhat higher freeze-out temperature $T_{\rm f} \approx 125\,{\rm MeV}$, with a 20% larger radial flow at RHIC than at the SPS at the same value of $T$.

## V. THE MISSING RHO: WATCHING THERMALIZATION

If the Little Bang started at initial energy densities above $3\,{\rm GeV/fm}^3$ , but decoupled only at about $50\,{\rm MeV/fm}^3$, how can we find out what happened in between? The $\rho$ meson provides a first answer: it can decay into $e^+e^-$ or $\mu^+\mu^-$ pairs which escape from the fireball without further interactions, and this $\rho$-decay clock ticks at a rate of $1.3\,{\rm fm}/c$, the $\rho$ lifetime. What I mean by this is that after one generation of $\rho$'s has decayed, a second generation is created by resonant $\pi\pi$ scattering, which can again decay into dileptons, etc. The number of extra dileptons with the invariant mass of the $\rho$ is thus a measure for the time in which the fireball consists of strongly interacting hadrons [ 21]. Obviously, $\rho$ mesons do not exist before hadrons appear in the fireball, so they won't tell us anything about a possible initial QGP phase. But they still allow us to look *inside* the strongly interacting hadronic fireball at a later stage, still long before the hadrons decouple.

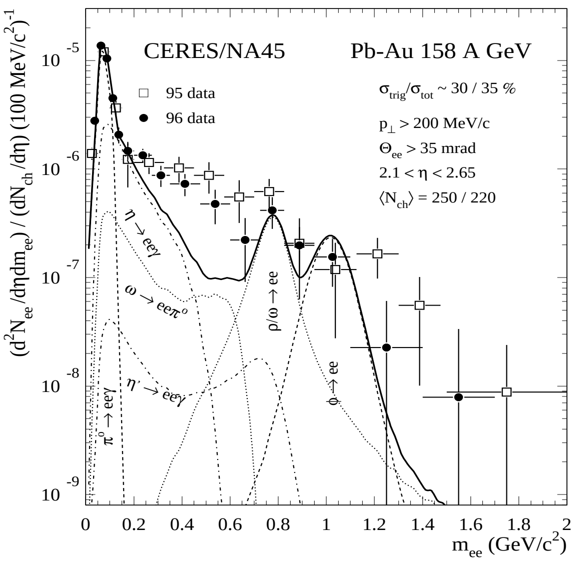


Figure 3. Invariant mass spectrum of $e^+e^-$ pairs from $158\,A\,{\rm GeV}/c$ Pb+Au collisions [ 22]. The solid line is the expected spectrum (the sum of the many shown contributions) from the decays of hadrons produced in $pp$ and $pA$ collisions (where it was experimentally checked [ 22]), properly scaled to the Pb+Au case. Two sets of data with different analyses are shown. Note that the $\rho$-peak reappears if only $e^+e^-$ pairs with $p_\perp > 500\,{\rm MeV}/c$ are selected [ 22]; such fast $\rho$'s escape quickly from the fireball and are not as strongly affected by collision broadening.

However, when the CERES/NA45 collaboration looked at the $e^+e^-$ spectrum in $158\,A\,{\rm GeV}/c$ Pb+Au collisions (see Fig. 3) and couldn't find the $\rho$ at all! They saw extra $e^+e^-$ pairs in the mass region of the $\rho$ and below (about 2.5–3 times as many as expected), but instead of a nice $\rho$-peak at $m_\rho = 770\,{\rm MeV}$ one sees only a broad smear [ 22]. Many explanations of the CERES-effect have been proposed, but the simplest one consistent with the data (for a review see [ 23]) is *collision broadening*: there is strong rescattering of the pions, not only among each other, but also with the baryons in the hadronic resonance gas, and this modifies their spectral densities and, as a consequence, leads to a smearing of the $\rho$-resonance in the $\pi\pi$ scattering cross section.

This demonstrates that, after first being formed in the hadronization process, the pions (the most abundant species at the SPS) undergo intense rescattering before finally freezing out. And this again is the mechanism which allows the fireball to reach and maintain a state of approximate local thermal equilibrium, to build up thermodynamic pressure and to collectively explode, as seen from the above analysis of the freeze-out stage. That the dileptons from collision-broadened $\rho$'s outnumber those from the decay of unmodified $\rho$'s emitted at thermal freeze-out (which should show up as a normal $\rho$-peak) shows that the hadronic rescattering stage must have lasted several $\rho$ lifetimes.

## VI. SEEING THE QUARK-HADRON TRANSITION

In the rest of this talk I will concentrate on observables which were found to differ drastically in AA and NN collisions but which we now believe cannot be changed efficiently by hadronic rescattering during the time between hadronization and kinetic freeze-out. Observables for which this can be firmly established yield insights about where AA and NN collisions differ already *before or during* hadronization, irrespective whether or not the hadrons rescatter after being formed.

One possibility how the early stage of an AA collision may differ from that in NN collisions is the formation of a quark-gluon plasma. I therefore review a few key QGP predictions and check how they fare in comparison with the data. In the present Section I discuss *strangeness enhancement* as a QGP signature, returning to two further QGP predictions in the following two Sections.

*Strangeness enhancement and chemical equilibration* were among the earliest predicted QGP signatures [ 24]. The idea is simple: 1. Color deconfinement leads to high gluon density, fostering $s\bar{s}$ creation by gluon fusion. 2. Chiral symmetry restoration renders the $s$-quarks relatively light, and in the QGP they can be created without the need for additional light quarks to make a hadron; both effects lower the production threshold. Both should considerably reduce the time needed for strangeness saturation and chemical equilibration compared to hadronic rescattering processes. Since in NN and $e^+e^-$ collisions strange hadron production is known to be suppressed relative to simple phase-space considerations [ 25], this should cause a relative strangeness enhancement in heavy-ion collisions.

Kinetic simulations based on known hadronic properties and interaction cross sections have shown that it is impossible to create a state of hadronic chemical equilibrium and a significant amount of strangeness enhancement out of a non-equilibrium initial state by purely hadronic rescattering [ 26]. If you want to get these features out, you have to put them in at the beginning of the simulation.

There may be many different ways of doing so, but the most efficient way of creating a state of (relative or absolute) hadronic chemical equilibrium may be provided by the hadronization process itself: If before hadronization the quarks and gluons are uncorrelated (such as in a QGP), then the most likely outcome of the non-perturbative hadronization process is a statistical occupation of the hadronic phase-space, a state of maximum entropy. If (as predicted for the QGP [

24]) the number of $s\bar{s}$-pairs is enhanced *before* the onset of hadronization, or by the fragmentation of gluons *during* hadronization, their statistical distribution over the available hadronic channels will naturally lead to an apparent hadronic chemical equilibrium state (with the corresponding enhancement of, say, the $\bar{\Omega}$) *even if none of the hadrons ever scattered with each other after being formed.*

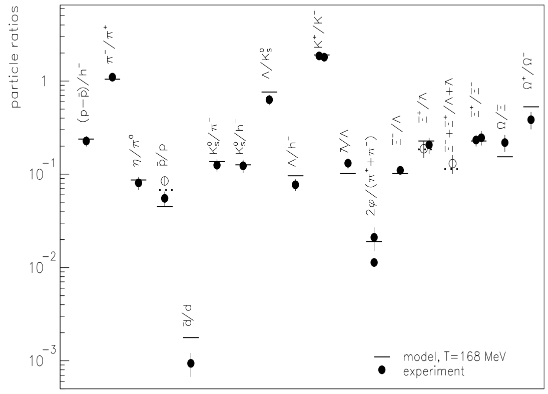


FIGURE 4. A compilation of measured particle ratios from 158 $A$ GeV/$c$ Pb+Pb collisions, compared with a hadron resonance gas in complete chemical equilibrium (full strangeness saturation) at $T_{\rm chem} = 168$ MeV and $\mu_{\rm B} = 266$ MeV [ 27].

Such a state of "apparent" or "pre-established" chemical equilibrium is indeed seen in the experiments: Fig. 4 shows 18 hadronic particle ratios from 158 $A$ GeV Pb+Pb collisions, compared with a hadronic chemical equilibrium state at $T_{\rm chem} = 168$ MeV and $\mu_{\rm B} = 266$ MeV [ 27]. A similar analysis of recent RHIC data [ 28] gives $T_{\rm chem} \simeq 175$ MeV and $\mu_{\rm B} \simeq 50$ MeV. The ratio of strange to non-strange quarks in the final hadrons is about a factor 2 higher than in *pp* collisions [ 29], and triply strange $\Omega$ baryons are enhanced relative to pBe collisions by a factor 17 [ 30]! This and the value of $T_{\rm chem}$ are interesting: $T_{\rm chem}$ characterizes the energy density at which hadronization occurs (about 0.5 GeV/fm$^3$) and coincides with the critical temperature for color deconfinement from lattice QCD. If the hadrons were formed by hadronization at the critical energy density $\epsilon_{\rm c}$ and their abundances froze out at $T_{\rm chem} \simeq 170$ MeV, there was no time to achieve this equilibrium configuration by hadronic rescattering; the hadrons must have been "born" into chemical equilibrium [ 31, 32]. Since subsequent hadronic rescattering is inefficient in changing the hadronic abundances [ 26], we can thus use them to measure $T_{\rm c}$.

## VII. $J/\psi$ SUPPRESSION AND COLOR DECONFINEMENT

What is the nature of the state from which the hadrons emerge in this manner? This question brings us to the second key QGP prediction [ 33]: the high gluon density resulting from color deconfinement should Debye-screen the color interaction between a $c$ and a $\bar{c}$ quark produced during the initial nuclear impact, thus preventing them from binding into charmonium states ($J/\psi$, $\chi_c$, $\psi$'). Instead, they would eventually find light quark partners to make hadrons with open charm. The result should be a suppression of charmonium production in heavy-ion collisions, and the screening mechanism should lead to a specific suppression pattern which, as a function of the achieved energy density, first affects the loosely bound $\psi$' and $\chi_c$ states and then the strongly bound $J/\psi$ ground state [ 34].

Nuclear $J/\psi$ suppression was indeed found at the SPS by the NA38/NA50 Collaboration. Fig. 5 shows that, as a function of collision centrality, measured by the produced transverse energy $E_T$ and in the left panel translated into an energy density at $\tau = 1\,\mathrm{fm}/c$ using a generalization of Eq. (1), the yield of $J/\psi$ mesons (identified by their $\mu^+\mu^-$ decay) is suppressed "anomalously" (i.e. below expectations). For a discussion of "normal" $J/\psi$ suppression I must refer to Refs. [ 34, 35]; it is well-defined and carefully experimentally tested and represented by the horizontal line in the left panel of Fig. 5. The observed deviation from this normal suppression is in qualitative agreement with the QGP prediction; in particular, the weakly bound $\psi'$ (not shown) already suffers anomalous suppression in central S+U collisions while the strongly bound $J/\psi$ shows it only in semicentral and central PbPb collisions. The observed pattern is not yet understood in all details [ 34, 36]; however, it definitely cannot be reproduced by final state rescattering of the $J/\psi$ with the dense hadronic environment after hadronization, represented by four independent calculations shown as lines in the right panel of Fig. 5.

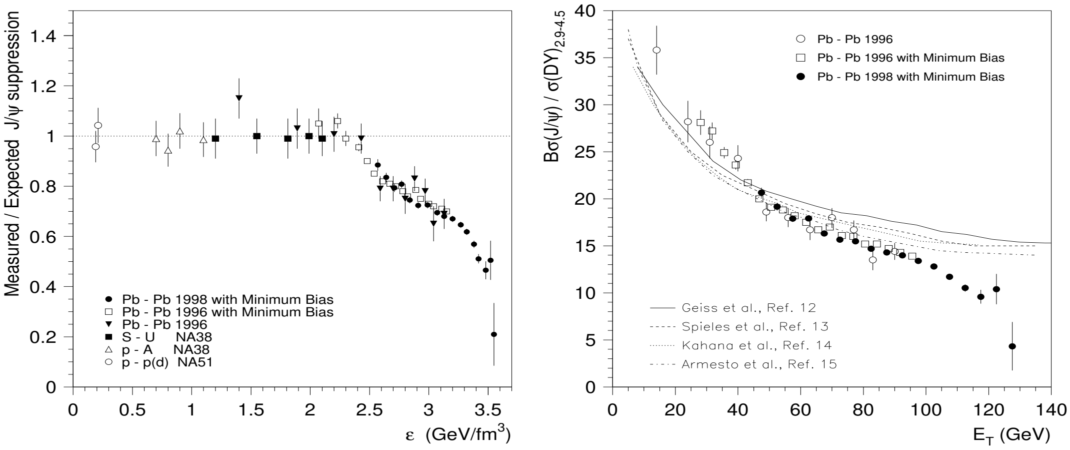


FIGURE 5. Left: "Anomalous $J/\psi$ suppression" as a function of initial energy density [ 35]. Right: The ratio $(J/\psi)$/Drell-Yan production, as a function of the measured transverse energy $E_T$, compared to hadronic comover models [ 35].

## VIII. THERMAL ELECTROMAGNETIC RADIATION

The third (and earliest) key prediction for QGP formation is thermal radiation of (real and virtual) photons from the thermalized quarks in the QGP [ 37]. In spite of the difficulties arising from large backgrounds, experiments at the SPS have searched for such radiation. In both the real [ 38] and virtual photon ($\mu^+\mu^-$ [ 39]) channels enhancements over hadronic decay backgrounds were reported. However, no unambiguous connection with thermal radiation has been established, in part because the predicted signal for the latter [ 40] is marginal at the SPS, given the accuracy of the experiments. To see the plasma "shine" one needs the higher temperatures and longer plasma lifetimes which can be reached at RHIC.

## IX. ELLIPTIC FLOW: AN EARLY HADRONIC SIGNATURE

In non-central heavy-ion collisions the initial overlap region is spatially deformed into an almond shape in the transverse plane. Nevertheless, at each point $\boldsymbol{r}$ the initial transverse momentum distribution is isotropic. If the produced matter expands without further interaction ("free streaming"), the $p_\perp$ distribution remains isotropic while the spatial deformation eventually disappears (the almond looks more spherical as it grows). On the other hand, if the produced matter thermalizes quickly, pressure builds up inside, and the spatial deformation results in anisotropic pressure gradients. These generate stronger collective flow in the shorter direction (i.e. into the reaction plane) than in the longer one (i.e. out of the reaction plane) [ 41], and the $p_\perp$-distribution becomes anisotropic. This phenomenon is called elliptic flow, measured by the second coefficient $v_2$ of an azimuthal Fourier decomposition of the $p_\perp$-spectrum [ 42]. Elliptic flow lets the almond grow faster along its short than along its long direction, thereby reducing its deformation. When the spatial deformation and the accompanying anisotropic pressure gradients vanish, $v_2$ stops growing. The higher the initial energy density, the longer the total fireball lifetime until hadronization and freeze-out, and the earlier this saturation occurs in the expansion history. This makes $v_2$ an *early signature* [ 43] (the more so the higher the initial energy density) which is carried by the abundant soft final state hadrons.

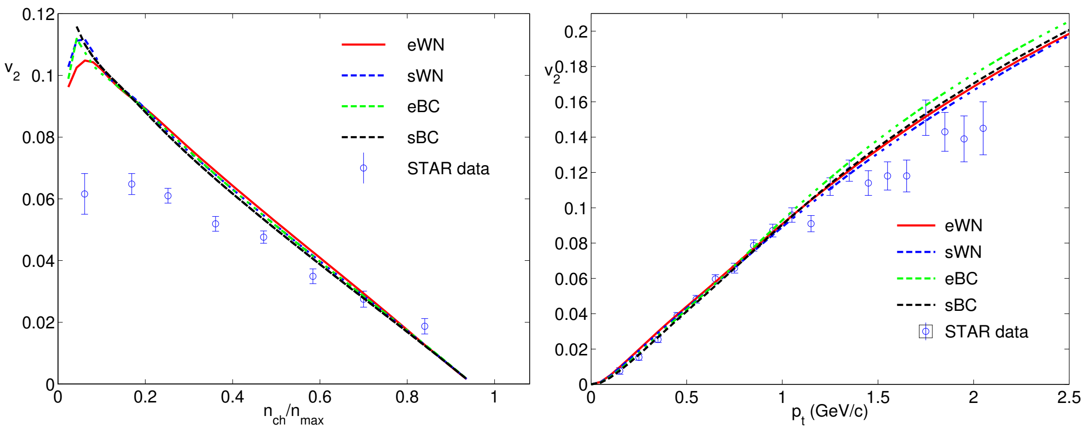


FIGURE 6. $p_\perp$ integrated elliptic flow coefficient $v_2$ as function of collision centrality (left) and differential elliptic flow $v_2(p_\perp)$ for minimum bias collisions (right) for 130 $A$ GeV Au+Au collisions at RHIC [ 46]. The curves are from hydrodynamic collisions with different initial density profiles [ 47].

Kinetic simulations [ 44] show that the momentum-space response to the spatial deformation grows monotonically with the interaction strength among the constituents of the produced matter. For a fixed spatial deformation, the largest $v_2$ response results from a system which is coupled so strongly that it thermalizes "instantaneously" on fluid dynamic time scales. This maximal response can thus be computed by solving the equations of ideal (non-viscous) hydrodynamics [ 41, 45]. Fig. 6 shows that the RHIC data exhaust this upper limit for semi-central

Au+Au collisions and low $p_\perp$, indicating very rapid thermalization on a time scale of 0.5 fm/$c$ [ 45]. For large impact parameters $b > 7\,\mathrm{fm}$ and $p_\perp > 1.5 - 2\,\mathrm{GeV}/c$ the measured $v_2$ stays below the hydrodynamic prediction, reflecting less efficient thermalization in small reaction volumes and at large transverse momenta. The hydrodynamic calculations show that the observed agreement between theory and data requires thermalization at energy densities well above $\epsilon_c$. It thus becomes difficult to avoid the conclusion that the prehadronic state formed in Au+Au collisions at RHIC is indeed a quark-gluon plasma.

## X. CONCLUSIONS

Relativistic heavy-ion collisions at the CERN SPS and RHIC have taken us into new and unprecedented regions of energy density, almost two orders above that of cold nuclear matter and well above the critical value for quark deconfinement. We have strong direct experimental evidence for a large degree of thermalization and strong collective behaviour setting in at a very early collision stage. Elliptic flow data show that at RHIC most of the anisotropic flow pattern is established before the energy density has dropped below $\epsilon_c$. This requires thermalization in the quark-gluon phase. Even at the SPS, the observed patterns of chemical equilibrium freeze-out at $T_c$ (now confirmed at RHIC), strangeness enhancement and $J/\psi$ suppression are fully consistent with predictions based on hypothetical QGP creation.

At the SPS the search for electromagnetic radiation directly emitted from the QGP phase did not provide convincing answers. The higher initial temperatures and longer plasma lifetimes at RHIC should make that task a bit easier, but we may still have to wait a while to see results. First tentative evidence for jet quenching at RHIC (see [ 48]) indicates that with this process we may have found another method of directly probing the early prehadronic collisions stage. The era of detailed studies of the properties of the QGP has now begun.

# REFERENCES


1. For a more detailed discussion see Rajagopal, K., these proceedings.
2. See Karsch, F., these proceedings.
3. Karsch, F., and Laermann, E., *Phys. Rev. D* **50**, 6954-6962 (1994).
4. Bjorken, J.D., *Phys. Rev. D* **27**, 140-151 (1983).
5. Alber, T., et al. (NA49 Collaboration), *Phys. Rev. Lett.* **75**, 3814-3817 (1995); Aggarwal, M., et al. (WA98 Collaboration), *Nucl. Phys.* **A610**, 200c-212c (1996); and *Eur. Phys. J. C* **18**, 651-663 (2001).
6. Adcox, K., et al. (PHENIX Collaboration), *Phys. Rev. Lett.* **87**, 052301 (2001).
7. Back, B.B., et al. (PHOBOS Collaboration), nucl-ex/0108009.
8. Kolb, P., et al., *Phys. Lett. B* **500**, 232-240 (2001).
9. Antinori, F., et al. (WA97 Collaboration), *Eur. Phys. J. C* **14**, 633-641 (2000).
10. Abreu, M.C., et al. (NA50 Collaboration), *Phys. Lett. B* **499**, 85-96 (2001).
11. van Hecke, H., Sorge, H., and Xu, N., *Phys. Rev. Lett.* **81**, 5764-5767 (1998).
12. Velkovska, J., et al. (PHENIX Collaboration), nucl-ex/0105012.

13. Harris, J., et al. (STAR Collaboration), Proceedings "Quark Matter 2001", Nucl. Phys. **A**, in press.
14. Huovinen, P., et al., *Phys. Lett. B* **503**, 58-64 (2001).
15. Chapman, S., Nix, J.R., and Heinz, U., *Phys. Rev. C* **52**, 2694-2703 (1995).
16. R. Scheibl and U. Heinz, Phys. Rev. C 59 (1999) 1585.
17. Murray, M., et al. (NA44 Collaboration), *Nucl. Phys.* **A661**, 456c-459c (1999).
18. Ambrosini, G., et al. (NA52 Collaboration), *New J. Phys.* **1**, 22 (1999).
19. Appelshäuser, H., et al. (NA49 Collaboration), *Eur. Phys. J. C* **2**, 661-670 (1998).
20. Tomášik, B., Wiedemann, U.A., and Heinz, U., nucl-th/9907096.
21. Heinz, U., and Lee, K.S., *Phys. Lett. B* **259**, 162-168 (1991).
22. Lenkeit, B., et al. (CERES Collaboration), *Nucl. Phys.* **A661**, 23c-32c (1999).
23. Rapp, R., and Wambach, J., *Adv. Nucl. Phys.* **25**, 1 (2000).
24. Rafelski, J., and Müller, B., *Phys. Rev. Lett.* **48**, 1066-1069 (1982); Koch, P., Müller, B., and Rafelski, J., *Phys. Rep.* **142**, 167-262 (1986).
25. Becattini, F., *Z. Phys. C* **69**, 485-492 (1996); Becattini, F., and Heinz, U., *ibid.* **76**, 269-286 (1997).
26. For a review see Heinz, U., *Nucl. Phys.* **A661**, 140c-149c (1999).
27. Braun-Munzinger, P., Heppe, I., and Stachel, J., *Phys. Lett. B* **465**, 15-20 (1999).
28. Braun-Munzinger, P., Magestro, D., Redlich, K., and Stachel, J., hep-ph/0105229.
29. Becattini, F., Gaździcki, M., and Sollfrank, J., *Eur. Phys. J. C* **5**, 143-153 (1998).
30. Lietava, R., et al. (WA97 Collaboration), *J. Phys. G* **25**, 181-188 (1999).
31. Heinz, U., *Nucl. Phys.* **A638**, 357c-364c (1998); *J. Phys. G* **25**, 263-274 (1999).
32. Stock, R., *Prog. Part. Nucl. Phys.* **42**, 295-309 (1999); *Phys. Lett. B* **456**, 277-282 (1999).
33. Matsui, T., and Satz, H., *Phys. Lett. B* **178** 416 (1986).
34. For a recent review see Satz, H., *Rep. Prog. Phys.* **63**, 1511-1574 (2000).
35. Abreu, M.C., et al. (NA50 Collaboration), *Phys. Lett. B* **477**, 28-36 (2000).
36. Blaizot, J.-P., Dinh, P.M., and Ollitrault, J.-Y., *Phys. Rev. Lett.* **85**, 4012-4015 (2000).
37. Shuryak,,E.V., *Phys. Lett.* **78B**, 150 (1978); Kajantie, K., and Miettinen, H.I., *Z. Phys. C* **9**, 341 (1981).
38. Aggarwal, M.M., et al. (WA98 Collaboration), *Phys. Rev. Lett.* **85**, 3595-3599 (2000).
39. Abreu, M.C., et al., (NA38 and NA50 Collaborations), *Eur. Phys. J. C* **14**, 443-455 (2000).
40. Gallmeister, K., Kämpfer, B., and Pavlenko, O.P., *Phys. Rev. C* **62**, 057901 (2000).
41. Ollitrault, J.-Y., *Phys. Rev. D* **46**, 229-245 (1992).
42. Voloshin, S.A., and Zhang, Y., *Z. Phys. C* **70**, 665-672 (1996).
43. Sorge, H., *Phys. Rev. Lett.* **78**, 2309-2312 (1997); *ibid.* **82**, 2048-2051 (1999).
44. Zhang, B., Gyulassy, M., and Ko, C.M., *Phys. Lett. B* **455**, 45-48 (1999); Molnar, D., and Gyulassy, M., nucl-th/0104073.
45. Kolb, P.F., Sollfrank, J., and Heinz, U., *Phys. Rev. C* **62**, 054909 (2000); Kolb, P.F., et al., *Phys. Lett. B* **500**, 232-240 (2001); Huovinen, P., et al., *ibid.* **503**, 58-64 (2001).
46. Ackermann, K.H., et al. (STAR Collaboration), *Phys. Rev. Lett.* **86**, 402-407 (2001).
47. Kolb, P.F., et al., *Nucl. Phys.* **A696**, 175-193 (2001).

48. Ullrich, T., these proceedings.